LETTER

doi:10.1038/nature09778

Interaction-based quantum metrology showing scaling beyond the Heisenberg limit

M. Napolitano[1], M. Koschorreck[1], B. Dubost[1,2], N. Behbood[1], R. J. Sewell[1] & M. W. Mitchell[1]

Quantum metrology aims to use entanglement and other quantum resources to improve precision measurement[1]. An interferometer using N independent particles to measure a parameter $\mathcal{X}$ can achieve at best the standard quantum limit of sensitivity, $\delta\mathcal{X} \propto N^{-1/2}$. However, using N entangled particles and exotic states[2], such an interferometer[3] can in principle achieve the Heisenberg limit, $\delta\mathcal{X} \propto N^{-1}$. Recent theoretical work[4–6] has argued that interactions among particles may be a valuable resource for quantum metrology, allowing scaling beyond the Heisenberg limit. Specifically, a k-particle interaction will produce sensitivity $\delta\mathcal{X} \propto N^{-k}$ with appropriate entangled states and $\delta\mathcal{X} \propto N^{-(k-1/2)}$ even without entanglement[7]. Here we demonstrate 'super-Heisenberg' scaling of $\delta\mathcal{X} \propto N^{-3/2}$ in a nonlinear, non-destructive[8,9] measurement of the magnetization[10,11] of an atomic ensemble[12]. We use fast optical nonlinearities to generate a pairwise photon–photon interaction[13] (corresponding to $k = 2$) while preserving quantum-noise-limited performance[7,14]. We observe super-Heisenberg scaling over two orders of magnitude in N, limited at large numbers by higher-order nonlinear effects, in good agreement with theory[13]. For a measurement of limited duration, super-Heisenberg scaling allows the nonlinear measurement to overtake in sensitivity a comparable linear measurement with the same number of photons. In other situations, however, higher-order nonlinearities prevent this crossover from occurring, reflecting the subtle relationship between scaling and sensitivity in nonlinear systems. Our work shows that interparticle interactions can improve sensitivity in a quantum-limited measurement, and experimentally demonstrates a new resource for quantum metrology.

The most precise instruments are interferometric in nature, and operate according to the laws of quantum mechanics. A collection of particles, for example photons or atoms, is prepared in a superposition state, allowed to evolve under the action of a Hamiltonian containing an unknown parameter, $\mathcal{X}$, and measured in agreement with quantum measurement theory. The complementarity of quantum measurements[15] determines the ultimate sensitivity of these instruments.

Here we describe polarization interferometry, used, for example, in optical magnetometry to detect atomic magnetization[11,16,17]; similar theory describes other interferometers[3]. A collection of N photons, with circular plus- and minus-polarization eigenstates, $|+\rangle$ and $|-\rangle$, is described by single-photon Stokes operators $\hat{s}_i = (1/2)(|+\rangle, |-\rangle)\sigma_i(\langle+|, \langle-|)^{\mathrm{T}}$, where σ_i ($i = x, y, z$) are the Pauli matrices, σ_0 is the identity and a superscript 'T' denotes transposition. In traditional quantum metrology, a Hamiltonian of the form $\hat{H} = \hbar\mathcal{X}\sum_{j=1}^{N}\hat{s}_z^{(j)}$, where $\hbar$ denotes Planck's constant divided by 2π, uniformly and independently couples the photons to $\mathcal{X}$, the parameter to be measured[1]. If the input state consists of independent photons, the possible precision scales as $\delta\mathcal{X} \propto N^{-1/2}$, the shot noise or standard quantum limit (SQL). The factor of $N^{-1/2}$ reflects the statistical averaging of independent results. In contrast, entangled states can be highly, even perfectly, correlated, giving precision limited by $\delta\mathcal{X} \propto N^{-1}$, the Heisenberg limit.

The above Hamiltonian is conveniently written $\hat{H} = \hbar\mathcal{X}\hat{S}_z$, where $\hat{S}_i \equiv \sum_{j=1}^{N}\hat{s}_i^{(j)}$ is a collective variable describing the net polarization of the photons. The independence of the photons manifests itself in the linearity of this Hamiltonian. Recently, it has been shown that interactions among particles, or, equivalently, nonlinear Hamiltonians, can contribute to measurement sensitivity and give scaling beyond the Heisenberg limit[4]. For example, a Hamiltonian $\hat{H} = \hbar\mathcal{X}\hat{S}_z^k$, that is, with a kth-order nonlinearity in $\hat{\mathbf{S}} \equiv (\hat{S}_x, \hat{S}_y, \hat{S}_z)$, contains k-photon interaction terms $\hat{s}_z^{(j_1)} \otimes \hat{s}_z^{(j_2)} \otimes \cdots \otimes \hat{s}_z^{(j_k)}$. The number of such terms, and, thus, the signal strength, grows as N^k, but the quantum noise from the input states is unchanged. As a result, a sensitivity limit of $\delta\mathcal{X} \propto N^{-k}$ applies when entanglement is used, and $\delta\mathcal{X} \propto N^{-(k-1/2)}$ in the absence of entanglement[7]. For $k \geq 2$, this gives scaling better than the Heisenberg limit, so-called super-Heisenberg scaling[7]. We note that interactions and entanglement are compatible and both improve the scaling. The predicted advantage applies generally to quantum interferometry, and proposed mechanisms to produce metrologically relevant interactions include Kerr nonlinearities[18], cold collisions in condensed atomic gases[7], Duffing nonlinearity in nanomechanical resonators[19] and a two-pass effective nonlinearity with an atomic ensemble[20]. Topological excitations in nonlinear systems may also give advantageous scaling[21].

In this Letter, we study interaction-based quantum metrology using unentangled probe particles. One challenge in demonstrating super-Heisenberg scaling is to engineer a suitable nonlinear Hamiltonian. Some nonlinearities have been shown to be intrinsically noisy[14] whereas others give super-Heisenberg scaling but fall short of the ideal, $\delta\mathcal{X} \propto N^{-(k-1/2)}$, under realistic conditions[7,22]. We use a cold atomic ensemble as a light–matter quantum interface[12] to produce quantum-noise-limited interactions, and use a Hamiltonian of the form $\hat{H} = \hbar\mathcal{X}\hat{S}_z\hat{S}_0 = \hbar\mathcal{X}\hat{S}_z N/2$. This Hamiltonian gives a polarization rotation that increases with photon number, without increasing quantum noise[7]. The experiment, shown schematically in Fig. 1, uses pulses of near-resonant light to measure the collective spin, $\hat{\mathbf{F}}$, of an ensemble of $N_{\mathrm{A}} \approx 10^6$ cold rubidium-87 atoms, probed on the $5S_{1/2} \rightarrow 5P_{3/2}$ D_2 line. The experimental system is described in detail in refs 8, 23. The on-axis atomic magnetization, $\langle\hat{F}_z\rangle$, which plays the role of $\mathcal{X}$ in this measurement, is prepared in the initial state $\langle\hat{F}_z\rangle = N_{\mathrm{A}}$ by optical pumping with resonant, circularly polarized light propagating along the trap axis, z. A weak, on-axis magnetic field is applied to preserve $\hat{F}_z$ during the measurements.

Pulses of $\hat{S}_x$-polarized, but not entangled, photons pass through the ensemble and experience an optical rotation proportional to $\langle\hat{F}_z\rangle$. The light–atom interaction Hamiltonian $\hat{H}_{\mathrm{eff}} = \alpha^{(1)}\hat{F}_z\hat{S}_z + \beta^{(1)}\hat{F}_z\hat{S}_z N/2$ describes this paramagnetic Faraday rotation[13]. Both the linear term, $\alpha^{(1)}\hat{F}_z\hat{S}_z$, and the nonlinear term, $\beta^{(1)}\hat{F}_z\hat{S}_z N/2$, cause rotation of the plane of polarization from $\hat{S}_x$ (vertical) towards $\hat{S}_y$ (diagonal). Detection of $\hat{S}_y$ then allows estimation of $\hat{F}_z$. As described in Supplementary Information, $\alpha^{(1)}$ and $\beta^{(1)}$ depend on the optical detuning, Δ, relative to the $F = 1 \rightarrow F' = 0$ transition; in particular, $\alpha^{(1)}(\Delta_0) = 0$

[1]ICFO-Institut de Ciencies Fotoniques, Mediterranean Technology Park, 08860 Castelldefels (Barcelona), Spain. [2]Laboratoire Matériaux et Phénomènes Quantiques, Université Paris Diderot et CNRS, UMR 7162, Bâtiment Condorcet, 75205 Paris Cedex 13, France.

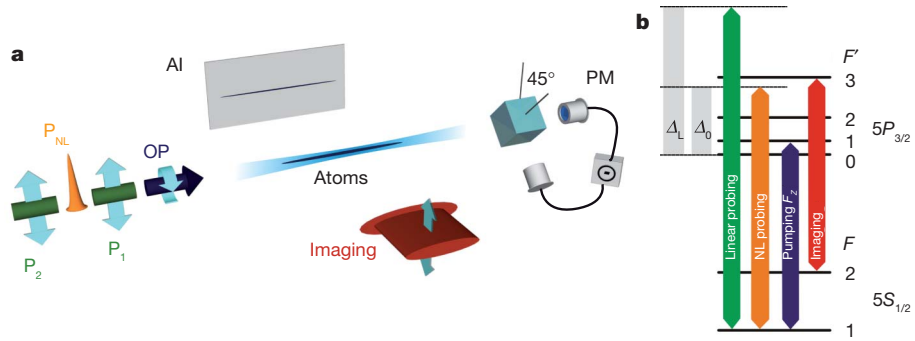

Figure 1 | Atom–light interface. **a**, Experimental schematic: an ensemble of 7×10^5 ^{87}Rb atoms, held in an optical dipole trap, is prepared in the state $|F = 1, m_F = 1\rangle$ by optical pumping (OP). Linear (P_1, P_2) and nonlinear (P_{NL}) Faraday rotation probe pulses (in the order P_1, P_{NL}, P_2) measure the atomic magnetization, detected by a shot-noise-limited polarimeter (PM). The atom number is measured by quantitative absorption imaging (AI). **b**, Spectral positions of the pump, probe and imaging light on the D_2 transition.

for the specific detuning $\Delta_0 \approx 2\pi \times 468.5$ MHz, allowing a purely nonlinear estimation to be studied.

The rotation angle is $\phi = \langle \hat{F}_z \rangle [A(\Delta) + B(\Delta)N]/2$, where $A \propto \alpha^{(1)}$ and $B \propto \beta^{(1)}$ both account for the temporal pulse shape and the geometric overlap between the atomic density and the spatial mode of the probe. The shot-noise-limited uncertainty in the rotation angle, due to quantum uncertainty in the initial angle, is $\delta\phi = N^{-1/2}/2$. A contribution, $\langle \hat{F}_z \rangle B(\Delta)\delta N/2$, from initial number fluctuations $\delta N = \langle N \rangle^{-1/2}$ is negligible for small rotation angles. This gives a measurement uncertainty of

$$\delta F_z = \langle \hat{F}_z \rangle \frac{\delta\phi}{\phi} = \frac{1}{A(\Delta)N^{1/2} + B(\Delta)N^{3/2}} \quad (1)$$

indicating a transition from SQL scaling, $\delta F_z \propto N^{-1/2}$, to super-Heisenberg scaling $\delta F_z \propto N^{-3/2}$ with increasing N.

We use two probing regimes. The 'linear probe' consists of 40 1-μs pulses (total illumination time, $\tau_L = 40$ μs) spread over 400 μs with detuning $\Delta_L \gg \Delta_0$. Together with the number of photons, N_L, used in the experiment for the linear probe, this gives $A \gg N_L B$, that is, linear estimation, and provides[8] a projection-noise-limited quantum non-demolition measurement[24] of $\hat{F}_z$, with uncertainty at the parts-per-thousand level[8]. The 'nonlinear probe' consists of a single, Gaussian-shaped, high-intensity pulse with a full-duration at half-maximum of $\tau_{NL} = 54$ ns, N_{NL} photons and a detuning Δ_0, such that $A \ll N_{NL}B$. Crucially, having two probes allows us to calibrate the nonlinear measurement precisely using a highly sensitive and well-characterized independent measurement of the same sample.

We probe the same sample three times for each preparation. First we use the linear probe, which gives a precise and non-destructive measurement of $\langle \hat{F}_z \rangle$ via the rotation angle, ϕ_L. Then we use the nonlinear probe, which gives a rotation angle, ϕ_{NL}, that is calibrated against the 'true' value (that is, with negligible error) provided by the linear probe. Finally we use a second linear probe to estimate the rotation angle $\phi_{L'}$, with which we can estimate the damage to the atomic magnetization, $\eta \equiv 1 - \phi_{L'}/\phi_L$, caused by the nonlinear probe.

The linear probe is calibrated using quantitative absorption imaging to measure N_A, and we find that $A(\Delta_L) = 3.3(1) \times 10^{-8}$ rad per atom. The calibration of the nonlinear probe against the first linear probe is shown in Fig. 2: We repeat the above pump–probe sequence while varying N_A in the range 1.5×10^5 to 3.5×10^5 to generate a ϕ_L-vs-ϕ_{NL} correlation plot for a given value of N_{NL}. Because both ϕ_L and ϕ_{NL} are linear in N_A, we use linear regression to find the slope, $b = d\phi_{NL}/d\phi_L = B(\Delta_0)N_{NL}/A(\Delta_L)$, for that value of N_{NL}. The experiment is repeated for a range of different N_{NL} values.

The observed plot of b versus N_{NL}, shown in Fig. 2a, is well fitted by a simple model including saturation of the nonlinear response:

$$\frac{d\phi_{NL}}{d\phi_L} = \frac{B(\Delta_0)N_{NL}}{A(\Delta_L)} \frac{1}{1 + N_{NL}/N_{NL}^{(sat)}} \quad (2)$$

Here $N_{NL}^{(sat)} = 6.0(8) \times 10^7$ is a saturation parameter and the nonlinear coupling strength is $B(\Delta_0) = 3.8(2) \times 10^{-16}$ rad per atom per photon.

The noise in the nonlinear probe, again as a function of N_{NL}, is determined from the ϕ_L-vs-ϕ_{NL} correlation plots. As illustrated in Fig. 2b, c, the residual standard deviation of the fits indicates the observed uncertainty, $\Delta\phi_{NL}$, which includes the intrinsic uncertainty, $\delta\phi_{NL}$, and a small contribution from electronic noise. In Fig. 3, we plot the fractional sensitivity, $\delta F_z^{(NL)}/\langle \hat{F}_z \rangle$, versus N_{NL}, calculated using equation (2) and considering the whole polarized ensemble, with $\langle \hat{F}_z \rangle = 7 \times 10^5$ spins. In agreement with equation (1), the log–log slope indicates the scaling $\delta F_z^{(NL)} \propto N_{NL}^{-3/2}$ to within experimental uncertainties in the range $N_{NL} = 10^6$ to 10^7, and super-Heisenberg scaling, that is, steeper than N^{-1}, over two orders of magnitude ($N_{NL} = 5 \times 10^5$ to 5×10^7).

Results of numerical modelling using the Maxwell–Bloch equations to describe the nonlinear light–atom interaction are also shown in Fig. 3. Two curves are shown, for detunings $\Delta_0 \pm (2\pi \times 200\,\text{kHz})$, covering the combined uncertainty in Δ due to the probe laser linewidth and inhomogeneous light shifts in the optical dipole trap. As expected from equation (1), this alters the sensitivity only at low N_{NL} values. The model is described in detail in Supplementary Information.

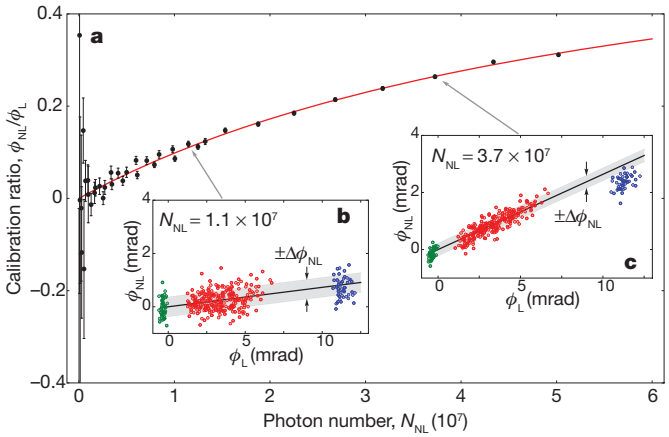

Figure 2 | Calibration of nonlinear Faraday rotation. **a**, Ratio of the nonlinear rotation, ϕ_{NL}, to the linear rotation, ϕ_L, versus the nonlinear probe photon number, N_{NL}. The data points and error bars indicate best-fit and standard errors from a linear regression, $\phi_{NL} = b\phi_L + \text{const.}$, for given values of N_{NL}. The red curve is a fit using equation (2), showing the expected nonlinear behaviour, $\phi_{NL} \propto N_{NL}$, with some saturation for large values of N_{NL}. **b**, **c**, ϕ_L-vs-ϕ_{NL} correlation plots for two values of N_{NL}. The atom number, N_A, is varied to produce a range of ϕ_L and ϕ_{NL} values. Green, no atoms ($N_A = 0$); red, $1.5 \times 10^5 < N_A < 3.5 \times 10^5$; blue, $N_A \approx 7 \times 10^5$. The blue circles are shown as a check on detector saturation, and are not included in the analysis.

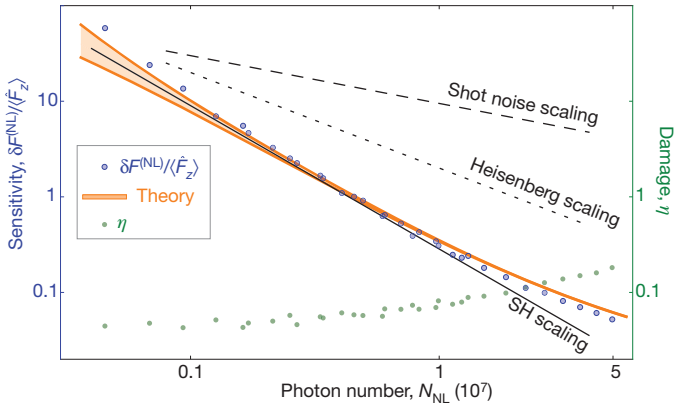

Figure 3 | Super-Heisenberg scaling. Fractional sensitivity, $\delta F_z^{(\mathrm{NL})}/\langle \hat{F}_z \rangle$, of the nonlinear probe plotted versus the number of interacting photons, N_{NL}. Blue circles indicate the measured sensitivity, orange curves show results of numerical modelling, and the black lines indicate SQL, Heisenberg-limit and super-Heisenberg (SH) scaling for reference. Scaling surpassing the Heisenberg limit, $\propto N_{\mathrm{NL}}^{-1}$, is observed over two orders of magnitude. The measured damage to the magnetization, η, shown as green circles, confirms the non-destructive nature of the measurement. Error bars for standard errors would be smaller than the symbols and are not shown.

For photon numbers above $N_{\mathrm{NL}} \approx 2 \times 10^7$, the saturation of the nonlinear rotation alters the slope. This can be understood as optical pumping of atoms into states other than $|F = 1, m_F = 1\rangle$ by the nonlinear probe. The damage to the atomic magnetization, $\eta = 1 - \phi_{\mathrm{L}'}/\phi_{\mathrm{L}}$, also shown in Fig. 3, remains small, confirming the non-destructive nature of the measurement. The finite damage even for small N_{NL} values is possibly due to stray light and/or magnetic fields disturbing the atoms during the 20-ms period between the two linear measurements. For large N, higher-order nonlinear effects including optical pumping limit the range of super-Heisenberg scaling.

The experimental results illustrate the subtle relationship between scaling and sensitivity in a nonlinear system. For an ideal nonlinear measurement, the improved scaling would guarantee better absolute sensitivity for sufficiently large N values. Indeed, when the measurement bandwidth is taken into account, the nonlinear probe overtakes the linear one at $N = 3.2 \times 10^6$, where both achieve a sensitivity of 1.1×10^2 spins $\mathrm{Hz}^{-1/2}$. As a consequence, the nonlinear technique performs better in fast measurements. In contrast, when measurement time is not a limited resource, the comparison can be made on a 'sensitivity-per-measurement' basis and the ideal crossover point, of 3.2×10^3 spins at $N = 8.7 \times 10^7$, is never actually reached, owing to the higher-order nonlinearities. Evidently, super-Heisenberg scaling allows but does not guarantee enhanced sensitivity: for the nonlinear technique to overtake the linear, it is also necessary that the scaling extend to large enough values of N. This example shows also that resource constraints dramatically influence the comparison between the linear and nonlinear techniques. See also Supplementary Information.

We have experimentally realized a system designed to achieve metrological sensitivity beyond the Heisenberg limit, $\delta\mathcal{X} \propto N^{-1}$, using metrologically relevant interactions among particles. To generate pairwise photon–photon interactions, we use fast, nonlinear optical effects in a cold atomic ensemble and measure the ensemble magnetization, $\langle \hat{F}_z \rangle$, with super-Heisenberg sensitivity $\delta F_z \propto N^{-3/2}$. To quantify the photon–photon interaction and the sensitivity rigorously, we calibrate against a precise, non-destructive, linear measurement of the same atomic quantity[8], demonstrate quantum-noise-limited performance of the optical instrumentation and place an upper limit on systematic, that is, non-atomic, nonlinearities at the level of a few per cent. The experiment demonstrates the use of interparticle interactions as a new resource for quantum metrology. Although possible applications to precision measurement will require detailed study, our experiment shows that interactions can produce super-Heisenberg scaling and improved precision in a quantum-limited measurement.

METHODS SUMMARY

Linear and nonlinear probe light. The probe beam is aligned on the axis of the trap with a waist of 20 μm, chosen to match the radial dimension of the cloud. In the linear probing regime, we use a train of 40 1-μs pulses, with a repetition rate of 100 kHz, each containing 3×10^6 photons detuned by +1.5 GHz from the $F = 1 \rightarrow F' = 0$ transition. The maximum intensity is 0.1 W cm^{-2}. The signals are summed and can be considered a single, modulated pulse.

The nonlinear probe consists of a single, Gaussian-shaped pulse with a full-duration at half-maximum of 54 ns. The maximum intensity of the nonlinear probe is 7 W cm^{-2} for a pulse with 10^7 photons. Theory predicts that $\alpha^{(1)} = 0$ at a detuning of $\Delta = 2\pi \times 462$ MHz in free space. This is modified by trap-induced light shifts, and we use the empirical value $\Delta_0 = 2\pi \times 468.5$ MHz, which gives zero rotation at low probe intensity.

Instrumental noise. The instrumental noise is quantified by measuring $\mathrm{var}(\hat{S}_y)$ versus input photon number N (that is, N_{L} or N_{NL}), in the absence of atoms, to find contributions from electronic noise ($V^{(\mathrm{el})} \propto N^0$), shot noise ($N^1$) and technical noise ($\propto N^2$), as described in Supplementary Information. We find that the contributions from electronic noise to the linear ($V_{\mathrm{L}}^{(\mathrm{el})}$) and nonlinear ($V_{\mathrm{NL}}^{(\mathrm{el})}$) probes are 3×10^5 and 4×10^5 per pulse, respectively, and that the technical noise is negligible. The instrumentation is thus shot-noise-limited over the full range of N used in the experiment. The intrinsic rotation uncertainty of the nonlinear probe, $\delta\phi_{\mathrm{NL}}$, is calculated from the measured $\Delta\phi_{\mathrm{NL}}$ as $(\delta\phi_{\mathrm{NL}})^2 = (\Delta\phi_{\mathrm{NL}})^2 - V_{\mathrm{NL}}^{(\mathrm{el})}$. The correction is at most 5%.

Instrumental linearity. The linearity of the experimental system and analysis is verified by using a wave plate in place of the atoms to produce a linear rotation equal to the largest observed nonlinear rotation. Over the full range of photon numbers used in the experiment, the detected rotation angle is constant to within 5%, and SQL scaling is observed.

Received 31 July; accepted 15 December 2010.

1. Giovannetti, V., Lloyd, S. & Maccone, L. Quantum metrology. *Phys. Rev. Lett.* **96,** 010401 (2006).
2. Mitchell, M. W., Lundeen, J. S. & Steinberg, A. M. Super-resolving phase measurements with a multiphoton entangled state. *Nature* **429,** 161–164 (2004).
3. Lee, H., Kok, P. & Dowling, J. P. A quantum Rosetta stone for interferometry. *J. Mod. Opt.* **49,** 2325–2338 (2002).
4. Boixo, S., Flammia, S. T., Caves, C. M. & Geremia, J. Generalized limits for single-parameter quantum estimation. *Phys. Rev. Lett.* **98,** 090401 (2007).
5. Choi, S. & Sundaram, B. Bose-Einstein condensate as a nonlinear Ramsey interferometer operating beyond the Heisenberg limit. *Phys. Rev. A* **77,** 053613 (2008).
6. Roy, S. M. & Braunstein, S. L. Exponentially enhanced quantum metrology. *Phys. Rev. Lett.* **100,** 220501 (2008).
7. Boixo, S. *et al.* Quantum metrology: dynamics versus entanglement. *Phys. Rev. Lett.* **101,** 040403 (2008).
8. Koschorreck, M., Napolitano, M., Dubost, B. & Mitchell, M. W. Sub-projection-noise sensitivity in broadband atomic magnetometry. *Phys. Rev. Lett.* **104,** 093602 (2010).
9. Koschorreck, M., Napolitano, M., Dubost, B. & Mitchell, M. W. Quantum nondemolition measurement of large-spin ensembles by dynamical decoupling. *Phys. Rev. Lett.* **105,** 093602 (2010).
10. Kominis, I., Kornack, T., Allred, J. & Romalis, M. A subfemtotesla multichannel atomic magnetometer. *Nature* **422,** 596–599 (2003).
11. Budker, D. & Romalis, M. Optical magnetometry. *Nature Phys.* **3,** 227–234 (2007).
12. Hammerer, K., Sørensen, A. S. & Polzik, E. S. Quantum interface between light and atomic ensembles. *Rev. Mod. Phys.* **82,** 1041–1093 (2010).
13. Napolitano, M. & Mitchell, M. W. Nonlinear metrology with a quantum interface. *N. J. Phys.* **12,** 093016 (2010).
14. Fleischhauer, M., Matsko, A. B. & Scully, M. O. Quantum limit of optical magnetometry in the presence of ac Stark shifts. *Phys. Rev. A* **62,** 013808 (2000).
15. Scully, M. O., Englert, B. G. & Walther, H. Quantum optical tests of complementarity. *Nature* **351,** 111–116 (1991).
16. Wasilewski, W. *et al.* Quantum noise limited and entanglement-assisted magnetometry. *Phys. Rev. Lett.* **104,** 133601 (2010).
17. Wolfgramm, F. *et al.* Squeezed-light optical magnetometry. *Phys. Rev. Lett.* **105,** 053601 (2010).
18. Beltrán, J. & Luis, A. Breaking the Heisenberg limit with inefficient detectors. *Phys. Rev. A* **72,** 045801 (2005).
19. Woolley, M. J., Milburn, G. J. & Caves, C. M. Nonlinear quantum metrology using coupled nanomechanical resonators. *N. J. Phys.* **10,** 125018 (2008).
20. Chase, B. A., Baragiola, B. Q., Partner, H. L., Black, B. D. & Geremia, J. M. Magnetometry via a double-pass continuous quantum measurement of atomic spin. *Phys. Rev. A* **79,** 062107 (2009).
21. Negretti, A., Henkel, C. & Mølmer, K. Quantum-limited position measurements of a dark matter-wave soliton. *Phys. Rev. A* **77,** 043606 (2008).

22. Boixo, S. *et al.* Quantum-limited metrology and Bose-Einstein condensates. *Phys. Rev. A* **80,** 032103 (2009).
23. Kubasik, M. *et al.* Polarization-based light-atom quantum interface with an all-optical trap. *Phys. Rev. A* **79,** 043815 (2009).
24. Braginskiĭ, V. B. & Vorontsov, Y. I. Quantum-mechanical limitations in macroscopic experiments and modern experimental technique. *Sov. Phys. Usp.* **17,** 644 (1975).

Supplementary Information is linked to the online version of the paper at www.nature.com/nature.

Acknowledgements We thank I. H. Deutsch and F. Illuminati for comments. We thank C. M. Caves and A. D. Codorníu for inspiration. This work was supported by the Spanish Ministry of Science and Innovation through the Consolider-Ingenio 2010 project QOIT, the Ingenio-Explora project OCHO (ref. FIS2009-07676-E/FIS) and project ILUMA (ref. FIS2008-01051), by the Marie-Curie RTN EMALI, and by Fundacio CELLEX Barcelona.

Author Contributions All authors contributed equally to the work presented in this paper.

Author Information Reprints and permissions information is available at www.nature.com/reprints. The authors declare no competing financial interests. Readers are welcome to comment on the online version of this article at www.nature.com/nature. Correspondence and requests for materials should be addressed to M.N. (mario.napolitano@icfo.es).